# Calculation of the influence of lateral chromatic aberration on image quality across the visual field

L. N. Thibos

*School of Optometry, Indiana University, Bloomington, Indiana 47405*

Received October 20, 1986; accepted March 31, 1987

The magnitude of lateral chromatic aberration and its effect on image contrast were computed for a modified, reduced-eye model of the human eye, using geometrical optics. The results indicate that lateral chromatic aberration is a major factor affecting image quality for obliquely incident rays of polychromatic light. Modulation transfer functions for white sinusoidal gratings decline monotonically with spatial frequency, with eccentricity of the stimulus in the peripheral visual field, with grating orientation relative to the visual meridian, and with decentering of the pupil. Image contrast is largely independent of the color temperature of white light over the range 2800 to 12,000 K, but it improves significantly for the polychromatic green light of the P-31 oscilloscope phosphor. Selective filtering by macular pigment increases image contrast by an amount that grows with spatial frequency to about a factor of 1.5 at the foveal resolution limit. Reduced contrast caused by lateral chromatic aberration accounts for most of the threefold loss of acuity that occurs for foveal viewing through a decentered pupil. The aberration probably has negligible effect on peripheral acuity but may act to limit aliasing of peripheral patterns.

## INTRODUCTION

Chromatic aberration of the eye is manifested in two ways. The first is a variation of the eye's focusing power with wavelength, referred to as axial or longitudinal chromatic aberration. The second is a prismatic dispersion of the spectrum, which is termed transverse or lateral chromatic aberration and may be thought of as a variation of angular magnification with wavelength. This prismatic effect arises when light rays strike a refracting surface obliquely, as when objects are viewed by peripheral vision or when the pupil is not centered on the optical axis of the eye. Whereas longitudinal chromatic aberration of the human eye has been widely studied since Newton, lateral chromatic aberration has not received much attention.[1] Helmholtz[2] commented that the colored border between a white and black field that results from chromatic aberration is hardly noticeable. Gullstrand[2] solidified this traditional view by arguing that although the magnitude of lateral chromatic aberration will increase with the retinal eccentricity of the image, at the same time, our ability to see the prismatic dispersion of the spectrum diminishes because of the relatively poor acuity of peripheral vision. Gullstrand's argument would not apply to foveal vision, of course, for which some effect of lateral chromatic aberration might have been expected because of the 5° horizontal eccentricity of the visual axis from the optical axis of the eye.[3] However, Le Grand[4] calculated that the angular dispersion of the visible spectrum is less than 3 arcmin for foveal vision and concluded that such a minor optical effect would play no visual role.

In retrospect, it seems surprising that the founders of physiological optics were so quick to dismiss the role of lateral chromatic aberration. Howarth,[5] who has extended Le Grand's calculations to include the whole of the visual field, points out that the size of the effect for foveal vision is more than an order of magnitude greater than both vernier acuity and stereo acuity and thus could be highly significant. Indeed, the perception of depth in a flat, multicolored pattern is due in part to the retinal disparity induced by lateral chromatic aberration.[6] Howarth's point is just as valid for peripheral vision. At 10° eccentricity, for example, vernier acuity is about 1–3 arcmin,[7,8] whereas the prismatic effect of lateral chromatic aberration is significantly larger, calculated[5] to be 6 arcmin over the visible spectral range from the Fraunhofer G line (0.43 $\mu$m) to the A line (0.77 $\mu$m).

The potential significance of lateral chromatic aberration for vision is not limited to hyperacuity tasks. Consider visual resolution of gratings. A 3 arcmin translation of a centrally viewed pattern represents more than a full cycle of spatial phase shift for gratings in the upper range (20–50 cycles/deg) of visible spatial frequencies. For polychromatic gratings, the phase shift of each spectral component of the retinal image varies with wavelength, and the net effect will be a loss of image contrast. The eye is not equally sensitive to all wavelengths, of course, so it is a matter for calculation to determine the loss of luminance contrast that results. This calculation has been done for the case of a decentered pupil,[9] and the result indicates that the loss of image contrast caused by lateral chromatic aberration is greater than the loss of contrast caused by coma or astigmatism, the other major off-axis aberrations. Furthermore, the optical factor appears to be more important than the Stiles–Crawford effect for determining visual contrast sensitivity, since it accounts for most of the threefold loss of foveal acuity that occurs when one is viewing through a decentered artificial pupil.[10]

In summary, contrary to earlier views, recent quantitative analysis suggests that lateral chromatic aberration may have profound effects on human visual performance and that these effects should vary systematically with stimulus eccentricity. Currently there is no quantitative description available to help to determine the adverse effects of lateral chro-

0740-3232/87/081673-08$02.00 

matic aberration across the full expanse of the visual field. This may be a more significant omission than previously thought because recent experiments have demonstrated that peripheral vision can detect the presence of gratings with high spatial frequencies far beyond the resolution limit.[11] For these reasons, the present study was undertaken to provide a full assessment of the effect of lateral chromatic aberration on image quality across the visual field.

## METHODS

Theoretical analysis of the effect of chromatic aberration on image contrast was conducted on an idealized model of the dioptrics of the eye by using the methods of geometrical optics. Gullstrand's reduced-eye model[2] is attractive because it has the same anterior and posterior focal lengths as more elaborate schematic eyes, yet it has only one refracting surface.[3] For it to be useful for the present calculations, however, two of the simplifying assumptions used to derive the reduced-eye model were abandoned. First, the index of the refracting medium, water, was permitted to vary with wavelength rather than being held fixed at the usual value of 4/3. This modification was required because a model with a fixed refractive index has no chromatic aberration. The second modification concerns the entrance and exit pupils. The limiting aperture of the Gullstrand model coincides with the refracting surface. It is shown below that this assumption causes an exaggeration of the magnitude of chromatic aberration, and so for present purposes it is more accurate to retain the entrance and exit pupils, as indicated in Fig. 1. Since there are no optical components after the pupil in this model, the exit pupil coincides with the natural pupil, which is 3.63 mm in front of the nodal point $N$. The entrance pupil is 10% larger than the natural pupil and is located 0.35 mm in front of the natural pupil or 3.98 mm in front of the nodal point and thus 3.25 mm behind the surface of the cornea of the real eye. The foregoing specification of the entrance pupil is for light with a wavelength of 0.57 $\mu$m. In fact, the location of the entrance pupil changes slightly with wavelength ($\pm$0.01 mm over the range 0.38–0.78 $\mu$m), but this small variation is ignored by the model.

Analysis begins with the construction of the chief ray, which joins a reference point on the grating object to the center P of the entrance pupil. The angle of incidence $\alpha$ is formed between the chief ray and the normal to the refracting surface, while eccentricity $\epsilon$ is that angle between the chief ray and the optical axis of the eye. The refracted chief ray emerges from the center of the exit pupil to form the angle $\gamma$ with the optical axis. The significance of the exit chief ray is that it defines the center of the dioptric blur circle formed in the image plane. This key attribute is important here because when chromatic aberration is present, only one wavelength can be focused at a time. By tracing the chief ray it is possible to specify the location of the image, even if it is out of focus, as a function of wavelength.

To determine the unknown exit angle $\gamma$, the usual paraxial approximation was avoided by finding the angle of incidence directly by the trigonometrical law of sines,

$$\sin(\alpha) = |\mathrm{NP}|\sin(180° - \epsilon)/R = 3.98\,\sin(\epsilon)/5.55, \qquad (1)$$

where $|NP|$ is the distance from the nodal point to the center of the entrance pupil. This permits the computation of the angle of refraction from Snell's law,

$$\sin(\beta) = \sin(\alpha)/n, \qquad (2)$$

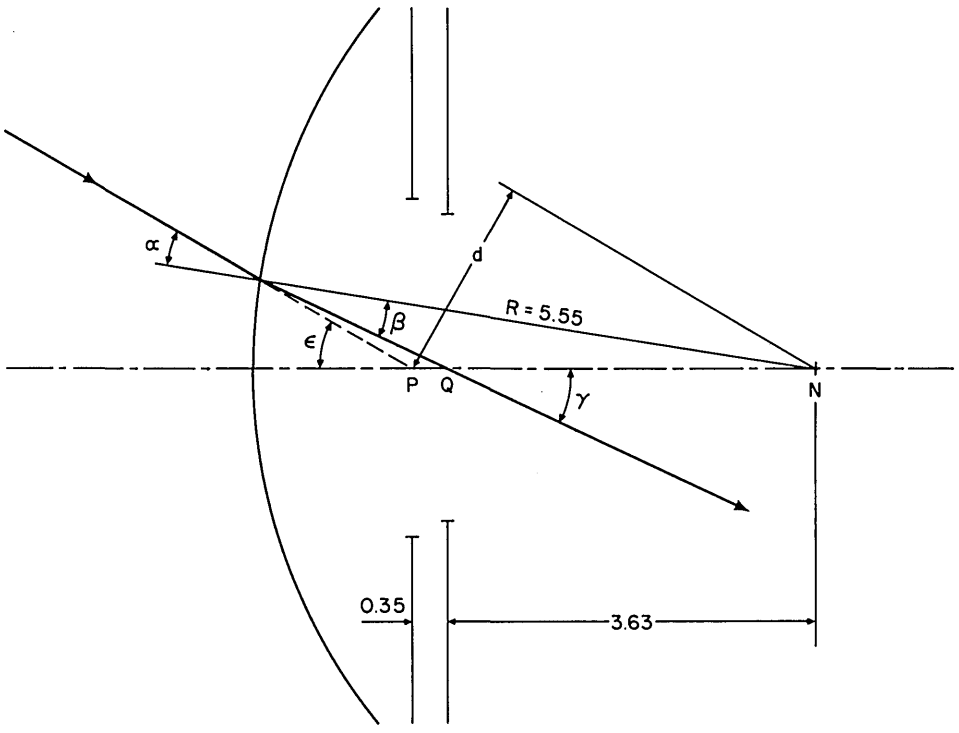


Fig. 1. Geometrical optics of the reduced-eye model of the human eye as modified to include the entrance and exit pupils. An incident chief ray of eccentricity $\epsilon$ is directed toward the center of the entrance pupil P and emerges from the center of the exit pupil at Q. The exit angle $\gamma$ varies with wavelength, thus inducing a change in image location and therefore a variable phase shift in the image of a polychromatic grating.

where $n$ is the index of refraction of the model eye. Cornu's formula for water given by Le Grand[4] was used to calculate the index of refraction as a function of wavelength $\lambda$ in micrometers:

$$n = 1.31848 + 0.0066620/(\lambda - 0.1292). \quad (3)$$

A more elaborate formula is also available,[12] but the differences are less than 0.001 in the visible spectrum.

The exit angle $\gamma$ is found from the geometry to be

$$\gamma = \epsilon - \alpha + \beta. \quad (4)$$

The angular magnification, $\gamma/\epsilon$, of this model is 0.82 when the index of refraction is 4/3, corresponding to $\lambda = 0.577$ $\mu$m by Eq. (3).

Lateral chromatic aberration is quantified by the change in exit angle $\lambda$ with wavelength for a fixed entrance angle. It is convenient to express this change in $\gamma$ relative to a reference angle $\gamma_0$, which is the exit angle for some reference wavelength. A choice of reference wavelength is arbitrary and inconsequential for the calculations of image contrast described below. The particular value chosen here is 0.57 $\mu$m, which is near the center of the visual spectrum and is the wavelength at which the index of refraction of water is 4/3. What is of primary importance for grating objects is that a change in the angle of the exit ray induces a spatial phase shift $\phi(\lambda)$ that varies with wavelength, with grating spatial frequency, and with grating orientation. Orientation is important because only the component of the angular shift in the direction orthogonal to the bars of the grating contributes to spatial phase. Let $\theta$ denote grating orientation relative to the visual meridian (e.g., $\theta = 0$ for horizontal gratings imaged on the horizontal meridian); then the phase shift induced by lateral chromatic aberration is given by

$$\phi(\lambda) = (\gamma - \gamma_0) f \sin(\theta)/0.82, \quad (5)$$

where $f$ is the spatial frequency of the grating in units of cycles per unit angle in object space as referenced to the entrance pupil. The image frequency, as referenced to the exit pupil, varies inversely with angular magnification. Strictly, since magnification varies with wavelength, so must image frequency. However, the change in frequency is less than 1% over the spectral range 0.38–0.78 $\mu$m. This fact permits the simplifying assumption that image frequency is independent of wavelength as provided by the fixed factor 0.82 in Eq. (5).

The image of a white grating is thus conceived as the sum of a multitude of gratings, each of the same spatial frequency but with a spatial phase that varies with wavelength. If $L(x, \lambda)$ is the luminance profile of the image in a direction $x$ orthogonal to the bars of the grating for wavelength $\lambda$, then each spectral component of the image is given by

$$L(x, \lambda) = S(\lambda)\{1 + M \cos 2\pi[fx - \phi(\lambda)]\}, \quad (6)$$

where $S(\lambda)$ is the mean luminance of the object at wavelength $\lambda$, whereas $M$ is object modulation, i.e., the grating contrast. $S(\lambda)$ takes into account the photopic spectral sensitivity curve of the eye and the spectral content of the object. Note that only the effects of lateral chromatic aberration are being considered here. Additional effects of diffraction and other aberrations are explicitly excluded from this analysis. Except where noted in relation to Figs. 5 and 6(a), all calculations reported here are for the CIE standard observer and a Planckian, blackbody radiator at 2800 K as tabulated by Moon.[13]

The luminance distribution of a polychromatic grating is found by integrating $L(x, \lambda)$ across wavelength:

$$L(x) = \int L(x, \lambda) d\lambda$$

$$= \int S(\lambda) d\lambda + M \int S(\lambda) \cos 2\pi[fx - \phi(\lambda)] \, d\lambda. \quad (7)$$

The first integral is just the mean luminance of the object, $L_0$. The second integral may be simplified by application of the trigonometric identity $\cos(X - Y) = \cos(X)\cos(Y) + \sin(X)\sin(Y)$ to yield

$$L(x) = L_0[1 + M\sqrt{A^2 + B^2} \cos(2\pi fx - Q)], \quad (8)$$

where $A$, $B$, and $Q$ are given by

$$A = \frac{1}{L_0} \int S(\lambda) \cos[\phi(\lambda)] d\lambda, \quad (9a)$$

$$B = \frac{1}{L_0} \int S(\lambda) \sin[\phi(\lambda)] d\lambda, \quad (9b)$$

$$Q = \arctan(B/A). \quad (9c)$$

The luminance equation [Eq. (8)] describes a grating image with modulation $M\sqrt{A^2 + B^2}$ and thus the ratio of image to object modulations is

$$\text{modulation transfer} = \sqrt{A^2 + B^2}. \quad (10)$$

Values of $A$ and $B$ were determined by numerical integration over the limits 0.38 to 0.78 $\mu$m in steps of 0.01 $\mu$m. All computations were done with the RS/1 programming system on a VAX-780 minicomputer.

## RESULTS

### The Magnitude of Lateral Chromatic Aberration

Lateral chromatic aberration of the reduced eye increases in magnitude with eccentricity, as shown in Fig. 2. The aberration is quantified here by the separation of images for a short wavelength (0.43 $\mu$m) and for a long wavelength (0.77 $\mu$m), which correspond to the blue and red ends of the visible spectrum (i.e. the G and A spectral lines). Calculations indicate that the aberration grows nearly linearly with eccentricity at the rate of about 0.28 min per degree of eccentricity. For foveal vision, assuming that the visual axis is 5° eccentric from the optical axis, this amounts to 1.4 min of angular separation, or about three times the diameter of an individual cone.

The assessment of lateral chromatic aberration shown in Fig. 2 is based on computed image locations for just two wavelengths of light. A more complete picture is shown in Fig. 3(a), in which the image displacement, relative to the reference wavelength of 0.57 $\mu$m, is shown as a function of wavelength for several eccentricities. All the curves decelerate, which means that the aberration is greater at the shorter wavelengths.

For grating objects, a displacement of the image induces a shift in spatial phase that is proportional to spatial frequen-

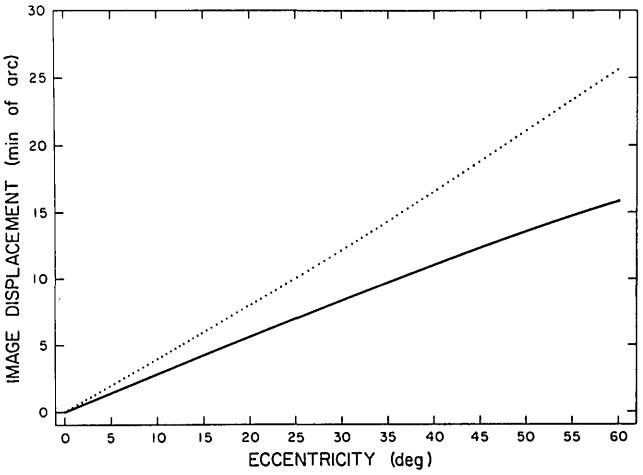


Fig. 2. Variation of lateral chromatic aberration with eccentricity. Solid curve shows the separation of images for wavelengths of 0.43 $\mu$m (Fraunhofer G line) and 0.77 $\mu$m (Fraunhofer A line) for the modified reduced eye of Fig. 1. Dotted curve shows this image separation for Gullstrand's reduced eye, which has the entrance and exit pupils at the refracting surface. The aberration is characterized in image space and referenced to the center of the exit pupil.

cy. Figure 3(b) shows this effect for gratings at a particular eccentricity (30°) from the optical axis. Although image displacements of only a few minutes of arc may at first seem insignificant, the corresponding phase shift can be considerable, depending on grating frequency. Calculated phase shifts in Fig. 3(b) are for gratings oriented orthogonal to the visual meridian (e.g., vertical gratings located on the horizontal meridian). No phase shift arises when gratings are parallel to the visual meridian because the direction of the displacement is parallel to the bars of the grating.

### The Effect of Lateral Chromatic Aberration on Image Contrast

The variable phase shift induced by chromatic aberration results in a loss of image contrast that varies with grating orientation, as shown in Fig. 4. Modulation transfer, which is the ratio of image contrast to object contrast, is unity for gratings oriented parallel to the visual meridian (relative orientation, 0°) and is minimized when the grating is orthogonal to the meridian (relative orientation, 90°). Between these two limits, contrast falls off smoothly with orientation. The rate of falloff increases with spatial frequency to such an extent that significant image contrast may be present for only a narrow range of relative orientations near zero. Since the effect of stimulus orientation is well ordered, further study of the effect of chromatic aberration on image contrast was confined to the worst case, that of gratings oriented orthogonal to the visual meridian.

Image contrast does not vary much with the color temperature of a white stimulus. Figure 5 illustrates the loss of image contrast with spatial frequency at a fixed eccentricity of 20° and a typical tungsten-light source (color temperature, 2800 K). Calculations were then repeated with all

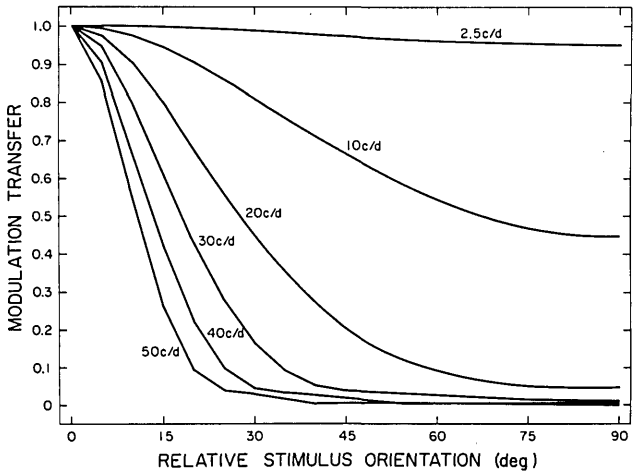


Fig. 4. The effect of lateral chromatic aberration on image contrast varies with grating orientation relative to visual meridian. $\epsilon = 30°$. The spatial frequency of each grating is indicated by a number near the curve [cycles per degree (c/d) in object space].

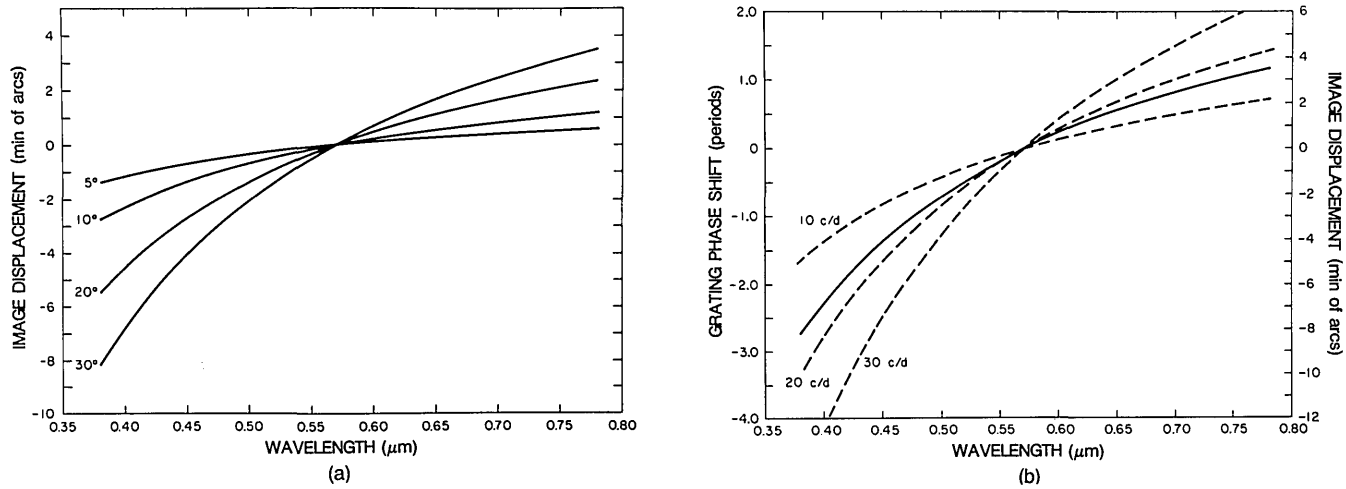


Fig. 3. (a) Image displacement and spatial phase shift across the visible spectrum of objects located at various eccentricities from the optical axis. Image position was calculated at 0.01-$\mu$m intervals, and the results are displayed relative to image position for the reference wavelength 0.57 $\mu$m. Numbers next to curves indicate object eccentricity ($\epsilon$) from the optical axis in degrees. (b) The effect of image displacement on spatial phase of gratings. Solid curve is the $\epsilon = 30°$ curve from (b) and is with reference to the right-hand ordinate. Dashed curves show the corresponding phase shift of gratings of various spatial frequencies and refer to the left-hand ordinate. Gratings are oriented orthogonal to visual meridian. c/d, Cycles per degree.

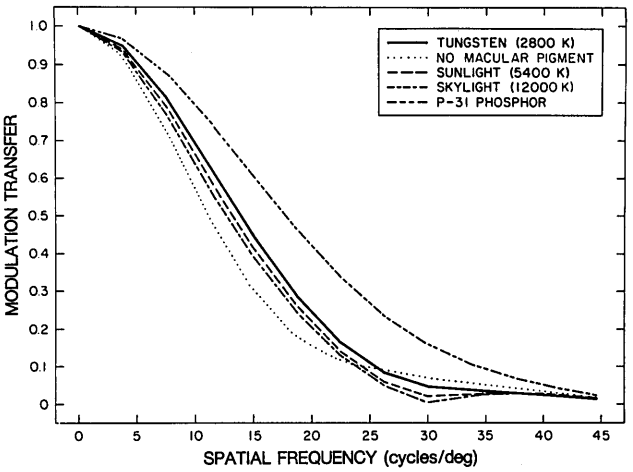


Fig. 5. Comparison of modulation transfer functions for various blackbody radiators and the P-31 oscilloscope phosphor, with $\epsilon$ = 20° and a relative orientation of 90°. The dotted curve shows the effect of removing macular pigment (tungsten source).

factors constant except the color temperature of the source. Results are displayed in Fig. 5 for sunlight and skylight, which have color temperatures of 5400 K and 12,000 K, respectively.[14] The differences between results for these blackbody radiators are small when compared with the significant improvement of contrast for an oscilloscope with the P-31 phosphor. This is due to the narrower spectrum of the oscilloscope light source.

Modulation transfer functions for selected values of eccentricity are shown in Fig. 6(a) for the tungsten source. Contrast falls off monotonically with spatial frequency, and this loss of image contrast becomes even greater the farther the stimulus moves into the peripheral field. The results are replotted in Fig. 6(b) to show the influence of eccentricity in greater detail. It must be remembered that these graphs show only the loss of contrast that is due to lateral chromatic aberration. Other aberrations, plus diffraction effects, will reduce contrast still further, but these additional factors have not been calculated here. The lack of macular pigment[15] in peripheral retina is another factor that will reduce image contrast still further. For these reasons, the curves of Fig. 6 are overestimates of the actual contrast of off-axis images.

## DISCUSSION

### Comparison with Previous Results

The magnitude of lateral chromatic aberration shown in Fig. 2, using the modified reduced eye (Fig. 1), is somewhat less than Howarth[5] calculated using the Gullstrand reduced eye, which has the entrance and exit pupils coincident with the refracting surface and centered on the optical axis. This difference was to be expected because the farther the entrance pupil is moved from the nodal plane toward the refracting surface, the greater will be the angle of incidence of the chief ray ($\alpha$ in Fig. 1) for a fixed eccentricity and, consequently, the greater will be the prismatic dispersion of the spectrum. To pursue this argument quantitatively, calculations were repeated for the Gullstrand reduced eye, and the results are shown by the dotted curve in Fig. 2. These values are close to those published by Howarth, with the remaining discrepancy accounted for by the fact that Howarth defined eccentricity as the angle of the exit ray of a representative wavelength, whereas in this paper eccentricity refers to the angle of the entrance ray. A comparison of the two curves of Fig. 2 indicates that Gullstrand's model exaggerates the magnitude of lateral chromatic aberration by about 50%.

Calculations reported here reveal a considerable loss of image contrast for white-light gratings in the peripheral field of view that occurs as a result of the spatial phase shift induced by lateral chromatic aberration. Contrast attenuation also occurs as a result of the focusing error known as longitudinal chromatic aberration. It is of interest to know which of these two facets of chromatic aberration has the

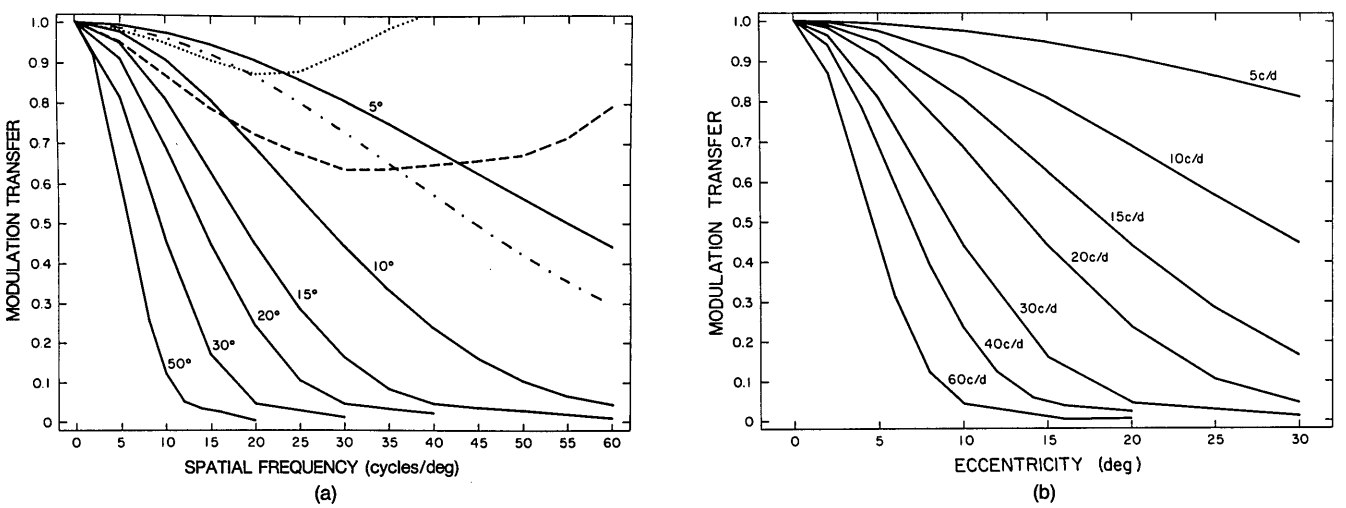


Fig. 6. Effect of lateral chromatic aberration on the modulation transfer function at different eccentricities. (a) Modulation transfer functions for selected eccentricities ($\epsilon$ is the number near each curve). The relative orientation is 90°, and the source color temperature is 2800 K. The dotted curve and the dashed curve show the loss of image contrast that is due to longitudinal chromatic aberration for 1.5- and 2.5-mm apertures, respectively (data are from Fig. 3 of Ref. 16). The dotted–dashed curve is for a pigment-free observer, with $\epsilon$ = 5°. (b) The same results are plotted as a function of eccentricity. The number near each curve indicates the spatial frequency in cycles per degree (c/d).

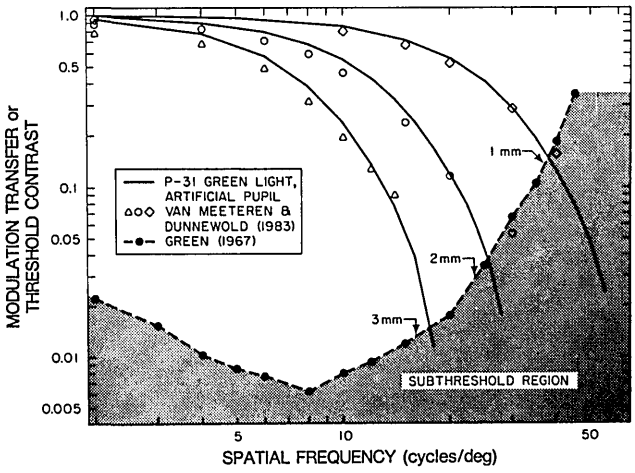


Fig. 7. Comparison of published calculations based on wave optics, psychophysical results for eccentric pupils, and present calculations based on geometrical optics. Symbols show the combined effects of lateral and longitudinal chromatic aberration for 1-mm (diamonds), 2-mm (circles) and 3-mm (triangles) translations of the entrance pupil computed by Van Meeteren and Dunnewold.[9] Solid curves are present results computed for lateral chromatic aberration only, assuming the spectrum of the P-31 phosphor, for the same three values of translation. The dashed curve is the contrast threshold function measured by Green[10] for foveal viewing of interference fringes. The intersections of dashed and solid curves give the predicted cutoff spatial frequencies for foveal viewing through artificial pupils decentered by 1, 2, and 3 mm. Arrows show the measured cutoff spatial frequencies determined psychophysically by Green for these same three values of pupil decentering.

greater influence of image contrast. In making the comparison it should be remembered that longitudinal chromatic aberration is independent of stimulus orientation and eccentricity, whereas lateral chromatic aberration varies strongly with both of these stimulus parameters. Published modulation transfer functions for longitudinal chromatic aberration[16] for 1.5- and 2.5-mm pupils are compared with present results in Fig. 6(a). Evidently, for white gratings oriented orthogonal to the visual meridian and located more than about 15° from the optical axis, lateral chromatic aberration has the greater effect on image contrast at all spatial frequencies.

Although the problem analyzed in the present paper is formulated in terms of objects located in the peripheral visual field, the solution applies equally well to the case of central vision through a decentered pupil. To see why, note that an eccentric viewing angle $\epsilon$ diagrammed in Fig. 1 corresponds to a lateral displacement $d$ of the pupil by the amount

$$d = |\mathrm{NP}|\sin(\epsilon) \qquad (11)$$

from an axis normal to the spherical refracting surface. Having established this correspondence between eccentricity and pupil displacement for the model, it becomes possible to compare the effects of lateral and longitudinal chromatic aberration another way. Van Meeteren and Dunnewold[9] used wave optics to calculate the combined effects of lateral and longitudinal chromatic aberration on the modulation transfer function of the reduced eye for the P-31 phosphor light source, and their results are shown by open symbols in Fig. 7. To compare these data with corresponding results obtained by geometrical optics, the isolated effect of lateral chromatic aberration was calculated for the Gullstrand model by using the present methods, and the results are shown by the solid curves of Fig. 7. For this model $NP = R$, and so 1, 2, and 3 mm of translation of the pupil correspond to 10.5°, 21°, and 33° of eccentricity, respectively. Evidently the combined effect of lateral and longitudinal chromatic aberration is only slightly greater than the effect of lateral chromatic aberration alone.

## The Effect of Lateral Chromatic Aberration on Central Vision

The optical analysis presented here provides the means for predicting the effect of lateral chromatic aberration on visual resolution when light enters the eye through different parts of the pupil. Predictions are made by comparing the loss of image contrast caused by lateral chromatic aberration with the sensitivity of the visual system to retinal image contrast. The necessary psychophysical estimates of the minimum retinal contrast necessary for pattern resolution were obtained by Green[10] from experiments in which monochromatic grating patterns were formed directly on the retina as interference fringes. Under these conditions, the variation of the threshold with spatial frequency defines the border between visible and invisible gratings in terms of retinal contrast, not of object contrast.

Threshold retinal contrast for Green's observer is shown by the dashed curve in Fig. 7. Retinal images with contrast values above the threshold function could be resolved by that observer; those below could not. Now when the observer views patterns generated on an oscilloscope, we predict that at some grating frequency, lateral chromatic aberration will reduce retinal image contrast below the threshold. This predicted acuity value is determined graphically in Fig. 7 by the intersections of the optical transfer functions with the psychophysical threshold function. For Green's observer, predicted acuity for 1, 2, and 3 mm of decentering are 38, 26 and 18 cycles/deg, respectively. Corresponding experimental determinations of acuity for this subject were 37, 24, and 16 cycles/deg, as indicated by the arrows in Fig. 7. This close agreement leaves little room for additional factors affecting visual resolution and firmly supports the conclusion of Van Meeteren and Dunnewold that lateral chromatic aberration is the major limiting factor for visual resolution of polychromatic gratings viewed through a decentered pupil.

## The Effect of Lateral Chromatic Aberration on Peripheral Vision

Although the effects of lateral chromatic aberration can be very large, it appears that peripheral visual acuity will not be significantly affected because the maximum resolvable spatial frequencies for peripheral vision are too low. Typical resolution limits for interferometrically produced gratings located 10°, 20°, and 30° into the periphery are about 10, 5, and 2.5 cycles/deg, respectively.[11,17] Lateral chromatic aberration would reduce image contrast by less than 7% in each case [Fig. 6(a)]. By the same argument, lateral chromatic aberration is probably not responsible for the finding that peripheral visual acuity varies systematically with stimulus orientation.[18-20]

Even though peripheral resolution of gratings may be relatively unaffected by lateral chromatic aberration, the same will not be true for peripheral detection of gratings. Recent

experiments have demonstrated that it is possible to see a grating that has a spatial frequency far beyond the classical resolution limit if the pattern is formed directly on the peripheral retina as interference fringes.[11] The visual percept that arises in this case is an erroneous one called aliasing.[21,22] In the light of these new experiments, it becomes important to know whether the optical aberrations of the eye would normally prevent the aliasing of high-frequency ratings in peripheral vision just as diffraction prevents aliasing in the fovea.[22] Present calculations indicate that lateral chromatic aberration would severely restrict the range of spatial frequencies subject to aliasing for gratings oriented orthogonal to the visual meridian but would have no effect on gratings oriented parallel to the visual meridian. This predicts an optically induced anisotropy in the detection of aliased patterns in the peripheral field, which has been experimentally verified.[23]

### Importance of Macular Pigment

It is widely believed that an important functional role of macular pigment is that of an optical filter that narrows the spectrum of the retinal image, thus protecting foveal vision from the deleterious effects of chromatic aberration.[15,24] To estimate the magnitude of this beneficial effect, calculations of image contrast were repeated for a hypothetical eye devoid of macular pigment. For these calculations to be made, the following two assumptions were required: (1) the fovea is 5° eccentric from the optical axis[3] and (2) the spectral sensitivity of a pigment-free standard observer equals the standard CIE sensitivity function divided by the transmission of the macular pigment. Recent evidence[25] suggests that the density of macular pigment is significantly higher than was previously thought, and so these higher values were used here to illustrate the greatest potential effect. The results, as shown by the dotted–dashed curve of Fig. 6(a), indicate that the presence of macular pigment significantly increases the image contrast by an amount that grows with spatial frequency to about a factor of 1.5 at 60 cycles/deg.

### Limitations of the Model

The calculations reported here do not take into account several relevant factors. The vertebrate lens is more dispersive than water,[26] and so the present results probably underestimate the magnitude of lateral chromatic aberration of the human eye. The magnitude of the error may not be large, however, judging from the close agreement of calculated and measured losses of acuity illustrated in Fig. 7. A more critical test of the water model, however, will require experimental measurements of lateral chromatic aberration in the human eye.

Since the calculations of this paper are based on the photopic spectral sensitivity curve for the CIE standard observer, they include the spectral transmission properties of the ocular media and macular pigment. Outside the macular region, one might expect the lack of macular pigment to be reflected in a broadening of the spectral sensitivity function. This in turn would lead to more severe attenuation of image contrast than has been calculated here. To gauge the importance of this factor, calculations for the tungsten source at 20° of eccentricity were repeated for the pigment-free standard observer as defined above. The results, as shown by the dotted curve in Fig. 5, indicate that removal of the macular pigment will significantly reduce the image contrast. The magnitude of the effect can be appreciated by noting that the transfer function for the standard observer viewing tungsten light lies about midway between the curves for the standard observer viewing P-31 light and the pigment-free observer viewing tungsten light. In other words, the loss of contrast that is due to the removal of macular pigment in the periphery is about equal to the gain of contrast after a change from white to polychromatic green light. This assessment is still only an approximation, however, as it ignores essential differences in the organization of central and peripheral retina such as the increased presence of both rods and short-wavelength cones in the periphery.[27–30]

The simplicity of the modified reduced eye makes it an attractive model for theoretical analysis of lateral chromatic aberration, but the limitations of simplified models must be acknowledged.[1] Real eyes have nonuniformities of refractive index of the cornea and lens, an accurate description of which would require more-sophisticated schematic eyes. Misalignment of the lens and cornea will make the optical axis ill defined. As the object moves farther into the peripheral visual field, the reduced-eye model becomes increasingly unrealistic.[31] On the other hand, idiosyncrasies of individual eyes will limit the predictive power of even the most elaborate model. Despite these uncertainties, the analysis presented here for a simple water model indicates that lateral chromatic aberration of the human eye is likely to be substantial and may play an important role in limiting the quality of vision throughout the visual field.

## ACKNOWLEDGMENTS

I thank A. Bradley, R. Everson, M. Campbell, and F. Cheney for helpful discussions of the issues and critical reviews of the manuscript and J. Kubley for graphics. This research was supported by National Institutes of Health grant EY5109.

## REFERENCES AND NOTES

1. W. N. Charman, "The retinal image in the human eye," Prog. Retinal Res. **2**, 1–50 (1983).
2. H. von Helmholtz, *Treatise on Physiological Optics* (with appendices by A. Gullstrand), J. P. C. Southall, ed. (Optical Society of America, Washington, D.C., 1924), Vol. 1.
3. H. H. Emsley, *Visual Optics*, 5th ed. (Hatton, London, 1952).
4. Y. Le Grand, *Form and Space Vision*, G. G. Heath and M. Millodot, eds. (Indiana U. Press, Bloomington, Ind., 1967).
5. P. A. Howarth, "The lateral chromatic aberration of the eye," Ophthalmol. Physiol. Opt. **4**, 223–226 (1984).
6. J. A. Sundet, "The effect of pupil size variations on the colour stereoscopic phenomenon," Vision Res. **12**, 1027–1032 (1972). Although this is best demonstrated with eccentric pupils, some individuals observe the illusion spontaneously, presumably because of the natural deviation of the pupillary axis from the optical axis.
7. R. D. Freeman, "Alignment detection and resolution as a function of retinal location," Am. J. Optom. Physiol. Opt. **43**, 812–817 (1966).
8. G. Westheimer, "The spatial grain of the perifoveal visual field," Vision Res. **22**, 157–162 (1982).
9. A. van Meeteren and C. J. W. Dunnewold, "Image quality of the human eye for eccentric entrance pupils," Vision Res. **23**, 573–579 (1983).
10. D. G. Green, "Visual resolution when light enters the eye through different parts of the pupil," J. Physiol. **190**, 583–593 (1967).

11. L. N. Thibos, F. E. Cheney, and D. J. Walsh, "Retinal limits to the detection and resolution of gratings," J. Opt. Soc. Am. A **4**, 1524–1529 (1987).
12. R. A. Houstoun, *A Treatise on Light*, 4th ed. (Longmans, Green, London, 1925).
13. P. Moon, *The Scientific Basis of Illumination Engineering* (Dover, New York, 1961).
14. J. W. T. Walsh, *The Science of Daylight* (Macdonald, London, 1961).
15. G. Walls, *The Vertebrate Eye and Its Adaptive Radiation* (Hafner, London, 1963).
16. F. W. Campbell and R. W. Gubisch, "The effect of chromatic aberration on visual acuity," J. Physiol. **192**, 345–358 (1967).
17. L. Frisen and A. Glansholm, "Optical and neural resolution in peripheral vision," Invest. Ophthalmol. **14**, 528–536 (1975).
18. D. J. Walsh and L. N. Thibos, "Oblique and meridional effects in peripheral vision," J. Opt. Soc. Am. A **2**(13), P65 (1985).
19. J. Rovamo, V. Virsu, P. Laurinen, and L. Hyvarinen, "Resolution of gratings oriented along and across meridians in peripheral vision," Invest. Ophthalmol. Vis. Sci. **23**, 666–670 (1982).
20. L. A. Temme, L. Malcus, and W. K. Noell, "Peripheral visual field is radially organized," Am. J. Optom. Physiol. Opt. **62**, 545–554 (1985).
21. L. N. Thibos, D. J. Walsh, and F. E. Cheney, "Vision beyond the resolution limit: aliasing in the periphery," submitted to Vision Res.
22. D. R. Williams, "Aliasing in human foveal vision," Vision Res. **25**, 195–205 (1985).
23. F. E. Cheney, "The effect of lateral chromatic aberration on the detection of gratings in peripheral vision," M.S. thesis (Indiana University, Bloomington, Ind., 1987).
24. V. M. Reading and R. A. Weale, "Macular pigment and chromatic aberration," J. Opt. Soc. Am. **64**, 231–234 (1974).
25. P. L. Pease, A. J. Adams, and E. Nuccio, "Optical density of human macular pigment," Vision Res. (to be published).
26. T. Mandelman and J. G. Sivak, "Longitudinal chromatic aberration of the vertebrate eye," Vision Res. **23**, 1555–1559 (1983).
27. R. A. Weale, "Spectral sensitivity and wave-length discrimination of the peripheral retina," J. Physiol. **119**, 170–190 (1953).
28. B. R. Wooten, K. Fuld, and L. Spillmann, "Photopic spectral sensitivity of the peripheral retina," J. Opt. Soc. Am. **65**, 334–342 (1975).
29. I. Abramov and J. Gordon, "Color vision in the peripheral retina. I. Spectral sensitivity," J. Opt. Soc. Am. **67**, 195–202 (1977).
30. B. Stabell and U. Stabell, "Spectral sensitivity in the far peripheral retina," J. Opt. Soc. Am. **70**, 959–963 (1980).
31. N. Drasdo and C. W. Fowler, "Non-linear projection of the retinal image in a wide-angle schematic eye," Br. J. Ophthalmol. **58**, 709–714 (1974).